HHMI Author Manuscript

HHMI Author Manuscript

HHMI Author Manuscript

Synthesis and Characterization of Degradable Bioconjugated Hydrogels with Hyperbranched Multifunctional Crosslinkers

Sara Pedrón[1,2], **Carmen Peinado**[1,*], **Paula Bosch**[1], and **Kristi S.Anseth**[3,4]

[1]Instituto de Ciencia y Tecnología de Polímeros, CSIC, Juan de la Cierva 3, 28006, Madrid, Spain Fax: (+34) 912 587 484

[3]Howard Hughes Institute, University of Colorado, Campus Box 424, Boulder, CO 80309, USA

[4]Department of Chemistry and Biological Engineering, University of Colorado, Campus Box 424, Boulder, CO 80309, USA

Abstract

Hyperbranched poly(ester amide) polymer (Hybrane™ S1200; M_n 1200 g/mol) was functionalized with maleic anhydride (MA) and propylene sulfide, to obtain multifunctional crosslinkers with fumaric and thiol-end groups, S1200MA and S1200SH, respectively. The degree of substitution of maleic acid groups (DS) was controlled by varying the molar ratio of MA to S1200 in the reaction mixture. Hydrogels were obtained by UV crosslinking of functionalized S1200 and poly(ethyleneglycol) diacrylate (PEGDA) in aqueous solutions. Compressive modulus increased with decreasing the S1200/PEG ratio and also depended on the DS of the multifunctional crosslinker (S1200). Also, heparin-based macromonomers together with functionalized hyperbranched polymers were used to construct novel functional hydrogels. The multivalent hyperbranched polymers allowed high crosslinking densities in heparin modified gels while introducing biodegradation sites. Both heparin presence and acrylate/thiol ratio have an impact on degradation profiles and morphologies. Hyperbranched crosslinked hydrogels showed no evidence of cell toxicity. Overall, the multifunctional crosslinkers afford hydrogels with promising properties that suggest that these may be suitable for tissue engineering applications.

Keywords

bioconjugated hydrogels; hyperbranched polymers; multifunctional crosslinkers; biodegradable; heparin

1. Introduction

Hydrogels are of widespread interest for applications in the pharmaceutical, biomedical1 and biotechnological fields.1,2 These materials offer a wide range of possibilities from drug delivery to wound healing due to their biocompatibility and resemblance to biological tissues.3,5 Recent trends in the development of *in situ* forming biomaterials have focused on

[*]Corresponding author. cpeinado@ictp.csic.es.
[2]*Current address*: Philips Research Laboratories, High Tech Campus 11, room p.255, 5656 AA Eindhoven - The Netherlands

preparing multifunctional monomers that contain reactive groups to form crosslinked scaffolds. The crosslinker plays an important role in determining the final swelling and pore size of the hydrogel matrix, thus making it an ideal target for synthetic modifications to control physical properties of hydrogels. The advantages of hyperbranched macromers for hydrogel formation include high crosslinking densities at low polymer concentrations, varied physical properties through judicious choice of the macromer structure, and low viscous aqueous solutions for injection in an *in vivo* site of irregular shape for subsequent crosslinking to form a well-integrated polymer network.[6] Low viscosities of the hydrogel precursors in water[7] can lead to gels with high solid contents and consequently excellent mechanical properties.[7]

Photopolymerization of multifunctional monomers is an efficient method applied for the preparation of hydrogels, allowing *in situ* formation of three-dimensional polymeric networks[9] in a minimally invasive manner.[10] However, it is possible that the network properties of the hydrogels may be affected by the polymerization conditions.[11,12] For example, it has been successfully applied for chondrocyte delivery to cartilage defects, promoting cell survival[13,14] and cartilage matrix synthesis.[15]

For many tissue regeneration applications, hydrogels are generally expected to degrade during or after tissue formation. The ideal hydrogel should degrade completely once the new tissue is formed.[16–20] The erosion of the material by degradation of the hydrogel is accompanied by changes in the physical properties, and this feature provides an opportunity to tune the biological response by selecting the desired shape of the mass loss profile.[20]

In this work, a polyamide ester (Hybrane™S1200) was explored as a crosslinker suitable for the fabrication of gels with tunable properties. First, gel degradation was pre-engineered by different approaches including selection of the chemistry and structure of the degradable blocks, along with the connectivity of the final network structure. Hydrogels fabricated through a thiolacrylate mixed-mode reaction scheme degrade hydrolytically at physiological pH through cleavage of ester linkages with the number of carbon atoms between the ester and sulfide groups affecting the rate of ester hydrolysis.[21] To incorporate biological functionality into the gel, heparin (Hp)[22] was incorporated as an enzymatically biodegradable component with the goal of promoting cell interactions and activity.

Here, we report the synthesis of two series of degradable crosslinked hydrogels, Hp-conjugated hydrogels and non-bioconjugated hydrogels. For this purpose, we synthesized two new types of crosslinkers based on a hyperbranched poly(ester amide) (Hybrane™ S1200). Their hydroxyl end-functionalities were modified to incorporate maleic or thiol moieties, and the photopolymerizable hyperbranched polymers were copolymerized with PEG diacrylate for the preparation of the hydrogels. The bioconjugated hydrogels, containing heparin, were prepared in the presence of (meth)acrylate-functionalized heparin following the same procedure. We selected a hyperbranched polymer possessing carboxylic ester functionalities in its backbone due to their well-understood mechanism of hydrolysis. Also, lower cytotoxicity is expected than that of low molecular weight crosslinkers, which are more readily internalized by cells. Mechanical properties and swelling behavior of these hydrogels were determined with varying composition and crosslinker concentration.

2. Materials and Methods

2.1. Materials

Hybrane™ S1200 ($\bar{M}_n$ 1200 Da) was kindly provided by DSM, The Netherlands. Heparin sodium salt from porcine intestinal mucosa (unfractionated, $\bar{M}_w$ 15 kDa), 4-(*N,N*-

dimethylamino) pyridine (DMAP), propylene sulfide, poly(ethyleneglycol) diacrylate ($\bar{M}_n$ 700 Da), triethylamine, acryloyl chloride, monoacrylate of poly(ethylene glycol) (M_n 375), succinic and maleic anhydrides and dicyclohexyl carbodiimide (1M in dichloromethane) were from Sigma Chemical Co. (St. Louis, MO). Glycidyl methacrylate (GMA) and poly(ethylene glycol) ($\bar{M}_n$ 4000 Da) were purchased from Fluka, *N*-hydroxysuccinimide (NHS) from Pierce and 2-Hydroxy-1-[4-(2-hydroxyethoxy) phenyl]-2-methyl-1-propanone (Irgacure 2959, purity 98%) was provided by Ciba Specialty Chemicals. CDCl$_3$ was supplied by Cambridge Isotopes. Chloroform and methylene chloride were from Scharlau and diethylether from SDS. Heparin-NHS was synthesis from heparin sodium salt as described previously.[23]

2.2. Synthesis

Synthesis of S1200MA—The hyperbranched polyol S1200 (3g, 2.5 mmol) was dissolved in chloroform (20% w/v). After the S1200 was clearly dissolved, maleic anhydride (1 g, 10 mmol) and a catalytic amount of DMAP (0.05 mol of the hydroxyl groups, 122 mg, 1 mmol) were added to the solution. Different amounts of maleic anhydride were added, 0.5 and 1.5 M respect to hydroxyl groups of S1200, in order to obtain different degrees of functionalization of the hyperbranched polymer. The reaction was conducted for 8 h at 60°C under nitrogen atmosphere. The reaction mixture was dialyzed against distilled water (Spectra/Por™ CE, MWCO 100) and lyophilized. The degree of substitution (DS, the number of derivatized hydroxyl groups) of the S1200MA samples was determined by ^{1}H NMR.

Synthesis of S1200SH—Thiol-end functionalized hyperbranched polymer was prepared by treating a 20% w/v solution of polyol (3g, 2.5 mmol) in distilled water with a 1.2 fold molar excess (respect to the concentration of hydroxyl groups, 24 mmol, 1.9 ml) of propylene sulfide at room temperature during 24h. After the reaction, the solution was dialyzed against distilled water (Spectra/Por™ CE, MWCO 500) and lyophilized.

Synthesis of poly(ethylene glycol) diacrylate—Poly(ethylene glycol) diacrylate (PEGDA, M_n 4000, 10 g, 2.5 mmol) was synthesized by reaction of PEG with acryloyl chloride (2 fold molar excess based on PEG hydroxyl end groups, 0.8 ml, 10 mmol), using triethylamine (equimolar with acryloyl chloride, 1.4 ml, 10 mmol) as a proton acceptor in methylene chloride. The acrylation efficiency (87%) was determined by ^{1}H NMR spectroscopy.

Heparin methacrylate (HpMA)—The incorporation of photopolymerizable methacrylate groups to heparin (Scheme 1) was carried out through the epoxide opening reaction of glycidyl methacrylate. Briefly, we prepared HpMA polymers by treating a 20% w/v solution of heparin (0.7 g, 3.4 mmol of hydroxyl groups) in distilled water with a 10 fold molar excess of glycidyl methacrylate (4.6 ml, 34 mmol) in the presence of a catalytic amount of hydrochloric acid (50 µl) at room temperature during 24h. After the reaction, the solution was dialyzed against distilled water (SpectraPore™ MWCO500) and lyophilized. The methacrylation efficiency was 60%, based on the ratio of the integrals for heparin protons and the terminal vinyl protons of the methacrylic moiety. The percentage of methacrylation refers to the number of methacrylate groups per heparin pentasaccharide unit.

Synthesis of PEG-acrylated heparin—In a first step heparin was modified with amine groups by 2 hours reaction of heparin-NHS (600 mg, 0.05 mmol) with ethylenediamine (5 fold molar excess of carboxylic groups, 4.8 mmol, 0.27 ml) in PBS pH 8.0 and purified by dialysis against water (Spectra/Por™ CE MWCO 500). The amine concentration per heparin

molecule was determined by Fluoraldehyde test (Fluoraldehyde™ Reagent Solution, Pierce, Rockford, IL). The result was a concentration of two free amino groups per heparin pentasaccharide, 80% of the total amount of present amines.

The poly(ethylene glycol) monoacrylate (M_n= 375 Da, 3.75 g, 10 mmol) and succinic anhydride (1.2 g, 12 mmol) were reacted in chloroform in the presence of a catalytic amount of DMAP (60 mg, 0.05 mmol), under nitrogen atmosphere at 60°C for 5 hours. The resulting product was washed with a solution of hydrochloric acid 1% v/v, dried and solvent was distilled off to obtain a white solid. The resulting product was dissolved in dichloromethane and reacted with *N*-hydroxysuccinimide (1.3 g, 11.5 mmol) in the presence of dicyclohexyl carbodiimide (40 ml 1M solution dichloromethane, 11.5 mmol) for 12 hours under inert atmosphere. Reaction stopped with the addition of 3 ml of distilled water, and the resulting urea derivative was filtered. After drying, solvent was evaporated by distillation under vacuum to obtain a white solid. The resulting product (0.11 g, 0.22 mmol) reacted with heparin (0.1 g, 0.009 mmol), previously modified with amine functional groups, in PBS pH 8.0 during 30 minutes at room temperature (Scheme 2). After dialysis for 48h, a white solid was obtained by lyophilization. The ^{1}H NMR integration of acrylate and PEG backbone peaks showed a modification of 30% (considering there is an average of two amine groups per heparin pentasaccharide that are susceptible for reaction with acrylated PEG).

Hydrogels preparation—Hydrogels were prepared by dissolving various amounts of modified hyperbranched crosslinker (from 5 to 15 wt %), poly(ethylene glycol) diacrylate and 0.5 wt% of Irgacure 2959 in PBS pH 6.5 at mass fraction of 25 wt%. The solution was photopolymerized between glass slides under UV light (Black Ray) at 365 nm and I_0=10 mW/cm^2 for 10 min (for PEG700DA) or 20 min (for PEG4000DA). Both sides of the gel were equally exposed to UV light to reach the maximum conversion of reactive groups according to rheological measurements. Table 1 collects the composition and physical characteristics of the different hydrogels prepared. Heparin conjugated hydrogels were prepared following the same procedure and using heparin monomers, methacrylate (**Hp2–7, 11–19**) or PEG-acrylate (**Hp8, 9** and **10**), to achieve concentrations from 0.1 to 10 mM for hydrogels with 25 wt% of solid content. Detailed composition and properties of these gels are given in Table 2.

A colorimetric reaction (*DMMB assay*) to detect glycosaminoglycans was used to measure the content of heparin in the gel networks.25

2.3. Characterization of gel samples

^{1}H NMR spectroscopy—^{1}H NMR spectra were recorded in D_2O and $CDCl_3$ on a Varian Inova-500 NMR spectrometer.

Size Exclusion Chromatography (SEC)—Molecular weights and polydispersity of heparin-based macromers were measured using a *Waters 1515 Isocratic HPLC Pump*, equipped with a precolumn, two serial connected columns (*Waters Ultrahydrogel™ 500* y *250*) and a refraction index detector (*Waters 2414*). Calibration was performed using polyethylene oxide standards. The elution phase used was acetonitrile/KNO_3 (0.1 M solution) (15:85 v/v), with a flow rate of 0.5 mL/min.

MALDI TOF—The modification of the S1200 polymer was analyzed by Matrix Assisted Laser Desorption/Ionization-Time of Flight. The analysis was carried out in a Voyager DE-PRO (Applied Biosystems, Foster City, CA, USA) mass spectrometer equipped with pulsed nitrogen laser (λ337 nm, 3 ns and 3 Hz). The positive ions generated by desorption passed a

flight tube (1.3 m) with an acceleration voltage of 25 kV. Spectra were obtained in the range of m/z 0.1–4 ku. Standards were angiotensin I, adrenocorticotrope hormone and bovine insulin.

Compression testing—The compression modulus of the hydrogels after photopolymerization and swelling was measured at room temperature using a mechanical testing machine MTS Bionix 100 (Model 810, MTS Systems Corp., Eden. Prairie, MN). After zeroing and taring the probe, sample disks of 4 mm diameter and 1.4 mm height were placed between parallel plates. Samples were compressed at a constant rate of 0.5 mm/s until a deformation of 20% was reached. The modulus (E) was calculated from the slope of the linear region of the curve at less than 10% deformation. Results are reported for data collected from at least 3 specimens for each material.

Swelling of hydrogels—In order to measure water absorption, disk-shaped hydrogels (5 mm diameter, 1 mm thickness) were prepared, transferred into pre-weighted glass vials and their initial weight (W_0) was recorded. Next, the vials were filled with 10 ml PBS pH 6.5 and pH 8.0. The hydrogel was removed at regular time intervals, surface water was gently removed with a paper towel and the hydrogel was then weighted (W_t) until no further weight change was detected. The instant swelling ratio is defined as the percentage ratio between the weight increase of the gel at time t and its initial weight ($[(W_t-W_0)/W_0]x100$). The swelling ratio at the equilibrium, q, is defined as the relation between the weight of the swollen hydrogel at the equilibrium and the weight of the dried hydrogel (W_s/W_d).[26]

Estimation of network parameters—Two methods utilized to elucidate the structure of hydrogels are equilibrium-swelling theory (that can be analyzed by the Flory-Rehner theory[27]) and rubber-elasticity theory.[28] In the present case, the average molecular weight between crosslinks (M_c) of hydrogel materials can be calculated with the following equation derived from the rubber elasticity theory neglecting chain ends (Eq. 1):

$$M_c = \frac{3\rho RT}{E},$$

where ρ is the specific density of the hydrogel (g/cm^3), R is the gas constant, T is the absolute temperature and E is the Young's modulus (Pa) obtained from the mechanical analysis data. The density of the hydrogel was estimated from the density of the PEGDA (1.12 g/mL), S1200 (1.1750 g/mL) measured by means of a helium picnometer, and the content of water of the hydrogel in the equilibrium swelling (1.0 g/mL). Defining crosslinking density, ν_e, as (Eq. 2):

$$\nu_e = \frac{E}{3RT}$$

Scanning Electron Microscopy (SEM)—To visually examine the surface and interior structure of the hydrogel in the swollen state, a *Philips XL-30* SEM was used (25 kV). The hydrogel samples were swollen in water for 24 h to reach equilibrium, and then quickly put into liquid nitrogen for ten minutes and transferred to a freeze-dryer for 72 h.

In vitro degradation of hydrogels—The degradation experiments were conducted at pH 7.4. The samples were weighed (W_t), subsequently immersed in the buffer and incubated at 37 °C. At different time intervals, some samples were taken out and mechanical properties were measured. The remaining samples were rinsed with deionized water, lyophilized, and

weighed as W_f. The percentage of remaining sample weight was calculated as $[W_f/W_t] \times 3100$.

Valvular Interstitial Cells (VICs) isolation and culture—VICs were isolated from porcine aortic valves[29] purchased from Quality Pork Processors Inc. (Austin, MN) by sequential collagenase digestion and cultured in growth media consisting of 15% FBS, 2% penicillin/streptomycin, 0.2% gentamicin in Media 199 (Invitrogen Corp.) at 37 °C in a 5% CO_2 environment. VICs were cultured at subconfluent densities and seeded on UV sterilized hydrogel disks at 50,000 cells/cm^2.

Statistics—Data were presented as mean ± standard deviation (SD). At minimum, three samples were represented for each data point. Data were compared using a two-tailed, unpaired *t*-test, and *p* values less than 0.05 were considered statistically significant.

4. Results and Discussion

4.1. Synthesis and characterization of hyperbranched crosslinkers

Different synthetic approaches have been used to obtain a new generation of crosslinkers by end-group functionalization of a commercial hyperbranched polymer. The introduction of a photopolymerizable group into hyperbranched S1200 was carried out following two different synthetic strategies, illustrated in Scheme 3. The synthesis of S1200MA was performed using a similar synthetic method as previously described for dextran modification.[30] The hydroxyl groups of the hyperbranched polyol reacted with the carbonyl group of maleic anhydride to form an ester linkage. This step also led to a ring opening of the anhydride group and generated a carboxylic acid group at the end of the attached segment. This mechanism preserves the functionality of the polymer irrespective of the DS and increases the hydrophilicity of hydrogels with the DS. The newly available carboxylic acid functional group can then be used in any further incorporation of drugs or other bioactive agents.

The degree of substitution of S1200 was determined by both ^{1}H NMR and MALDI TOF techniques, and a good agreement was found between both methods. Two hydrogels with different DS (2 and 5) were obtained by varying the molar ratio of MA to S1200 in the reaction mixture. For example, a DS value of 5 indicates that 5 out of 8 hydroxyl groups of a S1200 molecule are esterified with fumaric groups. Variations in the reaction conditions, such as temperature, molar ratio or time did not lead to a full conversion of hydroxyl groups. Formation of aggregates due to hydrogen-bond interactions and steric hindrance may explain a lower reactivity compared to other branched polymers containing hydroxyl end groups.

The addition of thiol groups to S1200 was carried out through the ring opening reaction of propylene sulfide in the presence of the hyperbranched polyol, resulting in a DS 2. FTIR spectra also confirmed the reaction of hydroxyl groups of the polyol with the thiirane showing a band at 2560 cm^{-1}, which is related to the stretching vibration of S-H bond. The novel hyperbranched crosslinkers were termed S1200MA and S1200SH, depending on the reactive final groups.

4.2. Hydrogel formation and characterization

Hydrogels were prepared by photocrosslinking of PEGDA with end-functionalized hyperbranched macromonomers (S1200MA and S1200SH) at different concentrations in the initial solution. Table 1 summarizes the composition of the precursor formulations and crosslinking density of the prepared hydrogels. Polymerization was photochemically

initiated using Irgacure 2959, which is water-soluble and cytocompatible.[31] The resulting S1200MA/PEGDA hydrogels were flexible and semitransparent whereas S1200SH/PEGDA gels were opaque and white; indicating that phase separation occurred in gels with propanethiol groups. While S1200MA copolymerized with PEG diacrylate by a classic chain-growth reaction, thiol-end modified S1200SH was incorporated to PEGDA through a mixed-mode polymerization mechanism, a combination of chain-growth and step-growth reactions, where both reactions are radically mediated. The unique structure of the thiol-acrylate evolved from the mixed-mode polymerization mechanism and was directly impacted by the thiol:acrylate ratios, transitioning from being more chain-like to more step-like as the thiol:acrylate ratio increased.[32]

The swelling behavior of these hydrogels, which influences solute transport and cell viability from a tissue engineering perspective,[33] was studied and results are shown in Figure 1. The water content at equilibrium also depends on the crosslinking density, which was directly related to the concentration of crosslinkable and total reactive groups (Table 1). The swelling ratio increases when the S1200SH crosslinker content is increased from 5 to 25wt%; by further increasing the concentration (up to 50 wt%), a slight decrease in the swelling ratio is observed. This behavior may be explained by the mixed mode polymerization, giving rise to a change of the network structure. The loss of transparency as increasing the concentration of S1200SH suggests that phase segregation and increased hydrophobicity limits swelling in these gels. This effect is also enhanced by the increase in the concentration of crosslinkable groups and the formation of a more compact structure. For hydrogels crosslinked with S1200MA, only a slight increase in the swelling degree is observed at the highest concentrations used here. In this case, the increase in the crosslinking density is compensated by the hydrophilicity coming from the carboxylic groups in the fumaric acid.

Figure 1 also compiles the compressive modulus of S1200SH and S1200MA hydrogels. The decline in the reactive groups is accompanied by a softening of the hydrogel structure; only gels with a high increase in the concentration of crosslinkable groups show a stiffer structure (**10** and **17**). The compressive modulus decreased from 5.8 MPa for hydrogel **1** (in the absence of S1200MA) to 3.4 MPa for hydrogel **10** (15 wt% S1200MA, DS 5). The modulus decreased as end-modified hyperbranched polymer concentration increased in all cases, independently of the end-group functionality and its degree of substitution. Hydrogel **13** presents higher crosslinking density and modulus when compared to hydrogel **1** as a consequence of an increase of thiol conversion.[35]

The swelling behavior of the hydrogels as a function of time is shown in Table 3, and their magnitudes depend on the functionality and nature of hyperbranched macromer along with the pH of the media. A maximum swelling ratio is achieved in pH 6.5 medium for S1200MA crosslinked hydrogels (**5** and **10**). At pH 6.5 a high proportion of carboxilic acid groups in the hydrogel are expected to be in the form of carboxylates since fumaric acid has pK_a values of approximately 3.5 and 4.5, and therefore, the resulting electrostatic repulsion in the polymer network cause the hydrogel to swell. At higher pH, counterions pair with the ionized carboxylic groups, resulting in a lower swelling ratio at pH 8.0. However, the hydrogel containing S1200SH (**15**) exhibited the highest swelling ratio in alkaline medium, which can be explained by a faster and irreversible degradation process in alkaline buffer. An increase in the swelling ratio of S1200MA crosslinked hydrogels (from **5** to **10**) is accompanied by a decrease in the time to reach equilibrium, irrespective of the pH of the medium. This is opposed to observations in hydrogels prepared by conventional crosslinking of vinyl groups,[34] and is explained by means of an increase in the hydrophilicity with the incorporation of maleic acid segments as the DS increases.

In order to study the network structure of the hydrogels, it was essential that certain aspects of the gel structure were determined.36 The average molecular weight between crosslinks (M_c) and the crosslinking density of the hydrogels at equilibrium swelling were calculated. The results of the estimated crosslinking density are given in Table 1 together with the crosslinkable acrylate and thiol groups concentration in the hydrogel precursor formulations. It should be noted that to calculate M_c, this model assumes that (i) the end-to-end distances of the chain are Gaussian, (ii) network deformation is affine and isothermal and (iii) dangling ends are absent. Likely, the hyperbranched networks do not fulfill these criteria and consequently, the presented data can only be considered in a relative way as reported elsewhere.37

Based on the above analysis, the thiol-ended crosslinkers led to hydrogels with higher crosslinking degree than those crosslinked with S1200MA using the same concentration of crosslinker with the same substitution degree. This result is more pronounced for low S1200SH concentration, and this fact agrees well with an enhancement of thiol conversion, as mentioned before. Increasing the molar concentration of thiol groups in the hydrogel formulation increases the amount of chain transfer occurring during polymerization, shortening the thiol-polyacrylate chains and reducing the number of crosslinks attached to each kinetic chain, which produces higher molecular weights between crosslinks. The introduction of multifuctional crosslinkers increases the number and the accessibility of functional groups available for reaction with PEG acrylate groups. Therefore, introduction of S1200MA hyperbranched macromer with DS5 would be expected to increase the crosslinking density, when compared to difunctional crosslinkers. Table 1 displays a general increase in ν_e when increasing the degree of substitution. Furthermore, both the unusual structure and high molecular weight of these hyperbranched crosslinkers play a key role in dictating the final network crosslinking density.38 In this regard, it should be noted the reduction of the total concentration of photoreactive groups by increasing the content of HBP DS 2 in the hydrogel formulations (Table 1). The latter gives rise to a decrease of ν_e as the hyperbrached crosslinker content increases. Further, these hydrogels composed of hyperbranched polymers may show no homogeneous structures compared to ideal crosslinked networks, presenting crosslink density gradients at a macroscopic level.39

Degradation of the hydrogels was carried out in PBS at pH 7.4 and 37°C. It was found that the weight loss profile was dependent on chemical composition (Figure 2). As the crosslinks were hydrolytically cleaved, the network crosslinking density decreased corresponding to an increase in the swelling ratio and a drop in the elastic modulus. Hydrogel **13** lost 25% of its mass after 25 days incubation and E decreased from 6.7 to 5.4 MPa, while no significant change was observed for hydrogel **1**, which does not contain the hyperbranched macromer, for the same period of incubation. These assays also reveal that gels with higher crosslinking densities exhibit higher degradation rates. The fastest mass loss of the hydrogel **13** compared with that of the other two hydrogels with the same content of hyperbrached crosslinker (**3** and **7**) is likely due to an easier dissociation of the hydrogel network and diffusion of the degradation products.

The increased liability of the S1200SH hydrogels is due to the presence of a thioether bond proximal to the acrylate ester bond. The presence of this moiety establishes a more positive atomic charge on the carbonyl carbon of the ester, enhancing its reactivity towards hydroxyl anions in base-catalyzed hydrolysis.40 Thus, gel **13** (ν_e=9.0) degraded 20% while gel **3** (ν_e= 5.7) lost only~10% of its weight in 25 days of incubation. The amount of HBP in the hydrogel formulation also modified degradability, hydrogels **7** and **13** made from 5 wt% of S1200MA (DS 5) and S1200SH, respectively, lost around 30% of their weights after 45 days, while gels with higher amounts of S1200MA or S1200SH (**5, 15** and **17**) only lost 5 to 10% over the same time of incubation. As explained previously, the increase in the

hyperbranched crosslinker concentration, leads to looser networks with fewer links to be cleaved before reaching reverse gelation (*i.e.*, complete dissolution).

Equilibrium swelling varies inversely to crosslinking density as degradation proceeds: when the ester bonds within the S1200 blocks hydrolyze, the crosslinking density decreases, and the network equilibrium swelling ratio increases. In 25 days of incubation, the equilibrium swelling ratios of S1200SH crosslinked gels increased depending on thiol concentration. Hydrogel **17**, which contains 50 wt% of S1200SH, shows a decline in the modulus with no mass loss, suggesting that crosslink cleavage occurs with no release of kinetic chains from the network due to the enhancement of final conversion.

4.3. Heparin-functionalized hydrogels: Formation and characterization

Heparin (Hp) was derivatized with methacrylate groups (Scheme 2) and incorporated to hydrogels via photopolymerization. Heparin-modified hydrogels were prepared using PEGDA of two molecular weights (700 and 4000 Da) and the end-functionalized hyperbranched macromers (Table 2). Hydrogels without HBP were prepared as a reference. Heparin incorporation to hydrogels was determined by a DMMB assay, suggesting an almost complete attachment of HpMA to the network (> 90%) in hydrogels **Hp2**–**7** and **Hp11**–**19**. However, incorporation of PEG-acrylated heparin in hydrogels **Hp8**–**10** was less than 50% for all concentrations due to the lower degree of functionalization of this macromonomer. Figure 3 shows the GPC chromatograms of the heparin macromers.

The presence of heparin, in S1200 crosslinked hydrogels, decreased water absorption at neutral pH while it was increased at pH 8.0, presented in Table 4. The chemical structure of heparin is characterized by the presence of carboxylic groups that confer sensitivity to pH, conditioning the total water uptake. At low pH more groups are protonated causing a reduction of electrostatic repulsions, giving rise to a more compact structure than that in basic media and therefore, hindering the swelling. Swelling experiments confirm the structure of the network envisaged on the basis of calculated crosslinking parameters (Table 2). The water content in the gels increase with heparin content, the more polar component, which contributes to a higher water uptake for bioconjugated gels. Heparin-modified hydrogels show lower crosslinking density, which should also favor water sorption in adequate pH solution. As an example, **Hp12** (10 mM Hp) showed an equilibrium swelling of 9.7 at pH 6.5 compared to 4.5 of **Hp11**, which contained 5mM Hp. By increasing the length of the PEG spacer using PEGDA, M_n 4000Da, the swelling ratio (q) is enhanced even for lower Hp contents (*i.e.*, **Hp4**, 0.1mM). Another interesting pattern is that the swelling ratio is independent of pH for these hydrogels, likely due to hindered electrostatic interactions by enlarging the distance between neighboring heparin moieties.

By increasing the amount of Hp the compressive modulus decreases for highly crosslinked hydrogels (**Hp1**, 4.3MPa to **Hp3**, 2.2MPa), as well for more loosely crosslinked hydrogels (**Hp4**, 444 kPa to **Hp7**, 85 kPa). In general, the presence of hyperbranched crosslinkers in the bioconjugated gels leads to a further reduction of the elastic modulus.

The modulus dramatically decreases when increasing the heparin/PEG ratio in the formulation. This effect is observed in all heparin gels, but the magnitude depends on the spacer chain between the polyacrylate and the polysaccharide, see PEG-acrylated heparin. The modulus of gel **Hp3** (10 mM heparin concentration) is half of that of **Hp2**, containing 10 times less the amount of heparin. Also, the spacer between the Hp molecules played an important role, and the decrease of E and increase of swelling ratio are not as marked in the PEG-acrylated heparin as in heparin methacrylate based hydrogels. For example, gel **Hp6** has a lower modulus and higher swelling ratio than gel **Hp10**, due to a reduction of the electrostatic repulsions between heparin molecules.

The general trend is that ν_e decreases as Hp content increases, with the exception of **Hp15** that showed the highest crosslinking density amongst HBP-crosslinked hydrogels. The presence of S1200MA leads to an improvement of mechanical properties in the most compliant gels composed of PEG4000 and high content of heparin, such as **Hp18** compared to **Hp6**. Degradation assays exhibit a higher loss of weight for gels **Hp1**, **Hp2** and **Hp3** in 45 days of incubation, when compared to gel **1**, see Figure 4. Also the addition of S1200MA to heparin hydrogels increas the degradation rate, deduced from the **Hp11** and **Hp12** data. Young modulus was also measured during the degradation process, and a good correlation was observed between the bulk degradation and mechanical property measurements (data not shown). The general trend follows the concentration of reactive groups in the formulation so that hydrogels having higher modulus appear more stable towards hydrolysis. **Hp13** showed the highest stability amongst the heparinized gels. Additionally, selective enzymatic degradation of these gels may allow tailored delivery of soluble heparin fragments, which may influence cell behavior.

4.4. Morphology of hydrogels

It is expected that hyperbranched nuclei with high segmental density may form a separated phase from the continuous one, composed mainly of linear chains and crosslink junctions. Figure 5 shows the micrographs of several hydrogel surfaces where differences in the network crosslinking density are evident. The hydrogels containing both heparin and end-functionalized hyperbranched macromer (Figure 5a–b) exhibit the presence of larger holes in the surface than those containing Hp or hyperbranched macromer. While both components define macroscopic structure, it can be deduced from Figure 5c and 5d that hyperbranched polymers have a major influence on porosity. The surface of gel **Hp3** with 10 mM heparin is rough while non-bioconjugated gels **7** and **10** have smoother surfaces and smaller pores (not shown in the figure). Regarding HBP content, the increase of hyperbranched macromers decreases the concentration of reactive groups in the medium as described previously. This decline in crosslinking density leads to the formation of less dense and more porous structures in non-bioconjugated hydrogels.

The physical properties and structural parameters, compiled in Tables 1 and 2, correlate well with the variation of the morphological features observed by SEM. Figure 6 shows the section micrographs of some selected hydrogels. These images depict the influence of the DS and reactive groups of the multifunctional crosslinker in the hydrogel structure, as well as the presence of heparin. The cross-sectional images of hydrogels containing only hyperbranched macromer (Figure 6a) or Hp macromer (Figure 6b) show a more compact morphology compared to those containing both Hp and hyperbranched macromers (Figures 6c–f). This result is in agreement with the observed surface morphology and also corresponds to hydrogels **3** and **Hp3** with higher crosslinking densities and lower degree of swelling compared to **Hp12**, **Hp14**, **Hp15** and **Hp19**. Crosslinking density of each hydrogel is included in the legend of the figure to envisage the impact of this parameter in the morphology. Moreover, it was observed that highly crosslinked hydrogel **8** (ν_e= 9) exhibited a very compact structure and, hydrogels containing hyperbranched crosslinker S1200MA with DS 2, formed less compact structure than that of hydrogel with S1200MA DS 5 (images not shown). Different behavior was observed for heparin containing hydrogels. When we looked at the cross section of the hydrogels **Hp12**, **Hp14**, **Hp15** and **Hp19**, larger pores were present in S1200SH hydrogels (Figure 6e–f) than S1200MA (Figure 6c–d). Although cell growth is believed to be affected by complex factors, the effect of scaffold pore size on cell growth has been previously reported.[42,43]

Preliminary studies about how this unusual crosslinked networks impact cell behavior show improved VIC-material interactions when poly(ethylene glycol) is copolymerized with

heparin and/or S1200MA (supplementary information). This initial cell-material interaction studies try to demonstrate how physico-chemical characteristics of this hydrogel materials can be tuned to promote cell attachment and morphology. Further, the presence of longer poly (ethylene oxide) chains in the network increases the porosity and gives rise to more compliant scaffolds. Thus, among all the gels tested hydrogel **Hp18**, prepared by photopolymerization of PEG4000DA, 10 wt% S1200MA (DS 2) and 10 mM HpMA, showed to promote desired VIC interactions.

5. Conclusions

In summary, we prepared novel biodegradable hydrogels based on PEG and a hyperbranched poly(ester amide) by UV photo-crosslinking. These hydrogels exhibit tunable properties, including swelling ratio, network parameters, and degradation rates depending on the crosslinker chemical structure and degree of substitution. This last parameter, DS, in hyperbranched macromers can be adjusted by tuning the ratio of maleic anhydride to the hyperbranched polymer S1200. The swelling ratio and network parameters change regularly with the hyperbranched polymer content, while the degradability of the hydrogels is highly related to the crosslinking density and pH conditions. On the other hand, the described gels were modified with heparin at different concentrations, leading to a decrease in crosslinking density. No significant cytotoxicity of the resulting gels was observed for valvular interstitial cells seeded on various formulations, and improved attachment and spreading occurred on more porous substrates, suggesting potential applications of these hydrogels as scaffolds for tissue engineering applications. Finally, the best results for VICs culture were obtained with bioconjugated hydrogels containing hyperbranched macromers, among the almost 40 hydrogels tested.

Supplementary Material

Refer to Web version on PubMed Central for supplementary material.

Acknowledgments

References

1. Peppas AN, Hilt JZ, Khademhosseini A, Langer R. Hydrogels in Biology and Medicine: From Molecular Principles to Bionanotechnology. Adv Mater. 2006; 18:1345–1360.

2. Drury JL, Mooney DJ. Hydrogels for tissue engineering: scaffold design variables and applications. Biomaterials. 2003; 24:4337–4351. [PubMed: 12922147]

3. Hubbell JA. Hydrogel systems for barriers and local drug delivery in the control of wound healing. J Control Release. 1996; 39:305–313.

4. Lutolf MP. Biomaterials: Spotlight on hydrogels. Nature Materials. 2009; 8:451–453.

5. Burdick JA. Bioengineering: Cellular control in two clicks. Nature. 2009; 460:469–470. [PubMed: 19626106]

6. Ifkovits JL, Burdick JA. Photopolymerizable and Degradable Biomaterials for Tissue Engineering Applications. Tissue Engineering. 2007; 13:2369–2385. [PubMed: 17658993]

7. Sunder A, Heinemann J, Frey H. Controlling the growth of polymer trees: concepts and perspectives for hyperbranched polymers. Chem Eur J. 2000; 6:2499–2506. [PubMed: 10961393]

8. Söntjens SHM, Nettles DL, Carnahan MA, Setton LA, Grinstaff MW. Biodendrimer-Based Hydrogel Scaffolds for Cartilage Tissue Repair. Biomacromolecules. 2006; 7:310–316. [PubMed: 16398530]

9. Oudshoorn MHM, Penterman R, Rissmann R, Bouwstra JA, Broer DJ, Hennink WE. Characterization of Structured Hydrogel Microparticles Based on Cross-Linked Hyperbranched Polyglycerol. Langmuir. 2007; 23:11819–11825. [PubMed: 17927225]

10. Elisseeff J, Anseth K, Sims D, McIntosh W, Randolph M, Langer R. Transdermal photopolymerization for minimally invasive implantation. Proc Natl Acad Sci USA. 1999; 96:3104–3107. [PubMed: 10077644]

11. Nguyen KT, West JL. Photopolymerizable hydrogels for tissue engineering applications. Biomaterials. 2002; 23:4307–4314. [PubMed: 12219820]

12. Kloxin AM, Anseth KS. Materials science: Protein gels on the move. Nature. 2008; 454:705–706. [PubMed: 18685693]

13. Du JZ, Sun TM, Weng SQ, Chen XS, Wang J. Synthesis and Characterization of Photo-Cross-Linked Hydrogels Based on Biodegradable Polyphosphoesters and Poly(ethylene glycol) Copolymers. Biomacromolecules. 2007; 8:3375–3381. [PubMed: 17902689]

14. Williams CG, Kim TK, Taboas A, Malik A, Manson P, Elisseeff J. In vitro chondrogenesis of bone marrow-derived mesenchymal stem cells in a photopolymerizing hydrogel. Tissue Engineering. 2003; 9:679–688. [PubMed: 13678446]

15. Kisiday J, Jin M, Kurz B, Hung H, Semino C, Zhang S, Grodzinsky AJ. Self-assembling peptide hydrogel fosters chondrocyte extracellular matrix production and cell division: implications for cartilage tissue repair. Proc Natl Acad Sci USA. 2002; 99:9996–10001. [PubMed: 12119393]

16. Nuttelman CR, Tripodi MC, Anseth KS. Dexamethasone-functionalized gels induce osteogenic differentiation of encapsulated hMSCs. J Biomed Mater Res Part A. 2006; 76A:183–195.

17. Halstenberg S, Panitch A, Rizzi S, Hall H, Hubbell JA. Biologically Engineered Protein-graft-Poly(ethylene glycol) Hydrogels: A Cell Adhesive and Plasmin-Degradable Biosynthetic Material for Tissue Repair. Biomacromolecules. 2002; 3:710–723. [PubMed: 12099815]

18. Bryant SJ, Anseth KS. Controlling the Spatial Distribution of ECM Components in Degradable PEG Hydrogels for Tissue Engineering Cartilage. J Biomed Mater Res. 2003; 64A:70–79.

19. Martens PJ, Bryant SJ, Anseth KS. Tailoring the Degradation of Hydrogels Formed from Multivinyl Poly(ethylene glycol) and Poly(vinyl alcohol) Macromers for Cartilage Tissue Engineering. Biomacromolecules. 2003; 4:283–292. [PubMed: 12625723]

20. Bryant SJ, Durand KL, Anseth KS. Manipulations in Hydrogel Chemistry Control Photoencapsulated Chondrocyte Behavior and their Extracellular Matrix Production. J Biomed Mater Res. 2003; 67A:1430–1436.

21. Nuttelman CR, Rice MA, Rydholm AE, Salinas CN, Shah DN, Anseth KS. Macromolecular monomers for the synthesis of hydrogel niches and their application in cell encapsulation and tissue engineering. Prog Polym Sci. 2008; 33:167–179. [PubMed: 19461945]

22. Rydholm AE, Anseth KS, Bowman CN. Effects of neighboring sulfides and pH on ester hydrolysis in thiol–acrylate photopolymers. Acta Biomaterialia. 2007; 3:449–455. [PubMed: 17276150]

23. Nilasaroya A, Poole-Warren LA, Whitelock JM, Martens PJ. Structural and functional characterisation of poly(vinyl alcohol) and heparin hydrogels. Biomaterials. 2008; 29:4658–4664. [PubMed: 18799212]

24. Zhou Z, Meyerhoff ME. Preparation and characterization of polymeric coatings with combined nitric oxide release and immobilized active heparin. Biomaterials. 2005; 26:6506–6517. [PubMed: 15941584]

25. Farndale RW, Buttle DJ, Barrett A. Improved quantitation and discrimination of sulfated glycosaminoglycans by use of dimethylmethylene blue. J Biochim Biophys Act. 1986; 883:173–177.

26. Flory, PJ. Principles of polymer chemistry. Cornell University Press; Ithaca, NY: 1953.

27. Langer R, Peppas NA. Advances in Biomaterials, Drug Delivery, and Bionanotechnology. AICHE J. 2003; 49:2990–3006.

28. Peppas NA, Bures P, Leobandung W, Ichikawa H. Hydrogels in pharmaceutical formulations. Eur J Pharm Biopharm. 2000; 50:27–46. [PubMed: 10840191]

29. Johnson C, Hanson M, Helgeson S. Porcine cardiac valvular subendothelial cells in culture: cell isolation and growth characteristics. J Mol Cell Cardiol. 1987; 19:1185–93. [PubMed: 3327949]

30. Kim SH, Won CY, Chu CC. Synthesis and characterization of dextran-maleic acid based hydrogel. J of Biomed Mater Res. 1999; 46:160–170. [PubMed: 10379993]

31. Bryant SJ, Nuttelman CR, Anseth KS. Cytocompatibility of UV and visible light photoinitiating systems on cultured NIH/3T3 fibroblasts in vitro. J Biomater Sci-Polym Ed. 2000; 11:439–457. [PubMed: 10896041]

32. Rydholm AE, Bowman CN, Anseth KS. Degradable thiol-acrylate photopolymers: polymerization and degradation behavior of an in situ forming biomaterial. Biomaterials. 2005; 26:4495–4506. [PubMed: 15722118]

33. Lee KY, Money DJ. Hydrogels for Tissue Engineering. Chem Rev. 2001; 101:1869–1879. [PubMed: 11710233]

34. Gonzales D, Fan K, Sevoian M. Synthesis and swelling characterizations of a poly(gamma-glutamic acid) hydrogel. J Polym Sci Part A: Polym Chem. 1996; 34:2019–2027.

35. Cramer NB, Bowman CN. Kinetics of thiol-ene and thiol-acrylate photopolymerizations with real-time Fourier transform infrared. J Polym Sci Part A: Polym Chem. 2001; 39:3311–3319.

36. Peppas, N., editor. Hydrogels in Medicine and Pharmacy. CRC; Boca Raton, FL: 1987.

37. Oudshoorn MHM, Rissman R, Bouwstra JA, Hennink WE. Synthesis and characterization of hyperbranched polyglycerols hydrogels. Biomaterials. 2006; 27:5471–5479. [PubMed: 16859743]

38. Pedron S, Bosch P, Peinado C. Using hyperbranched macromers as crosslinkers of methacrylic networks prepared by photopolymerization. J Photochem Photobiol A: Chem. 2008; 200:126–140.

39. Lin H, Wilen CE. Hyperbranched polymers with maleic functional groups as radical crosslinkers. J Polym Sci Part A: Polym Chem. 2001; 39:964–972.

40. Van de Wetering P, Metters AT, Schoenmakers RG, Hubbell JA. Poly(ethylene glycol) hydrogels formed by conjugate addition with controllable swelling, degradation, and release of pharmaceutically active proteins. J. Control Release. 2005; 102:619–627. [PubMed: 15681084]

41. Schultz KM, Baldwin AD, Kiick KL, Furst EM. Gelation of Covalently Cross-Linked PEG—Heparin Hydrogels. Macromolecules. 2009; 42:5310–5316. [PubMed: 21494422]

42. Dubruel P, Unger R, Vlierberghe SV, Cnudde V, Jacobs PJ, Schacht E, Kirkpatrick CJ. Porous Gelatin Hydrogels: 2. In Vitro Cell Interaction Study. Biomacromolecules. 2007; 8:338–344. [PubMed: 17291056]

43. Wachiralarpphaithoon C, Iwasaki Y, Akiyoshi K. Enzyme-degradable phosphorylcholine porous hydrogels cross-linked with polyphosphoesters for cell matrices. Biomaterials. 2007; 28:984–993. [PubMed: 17107708]
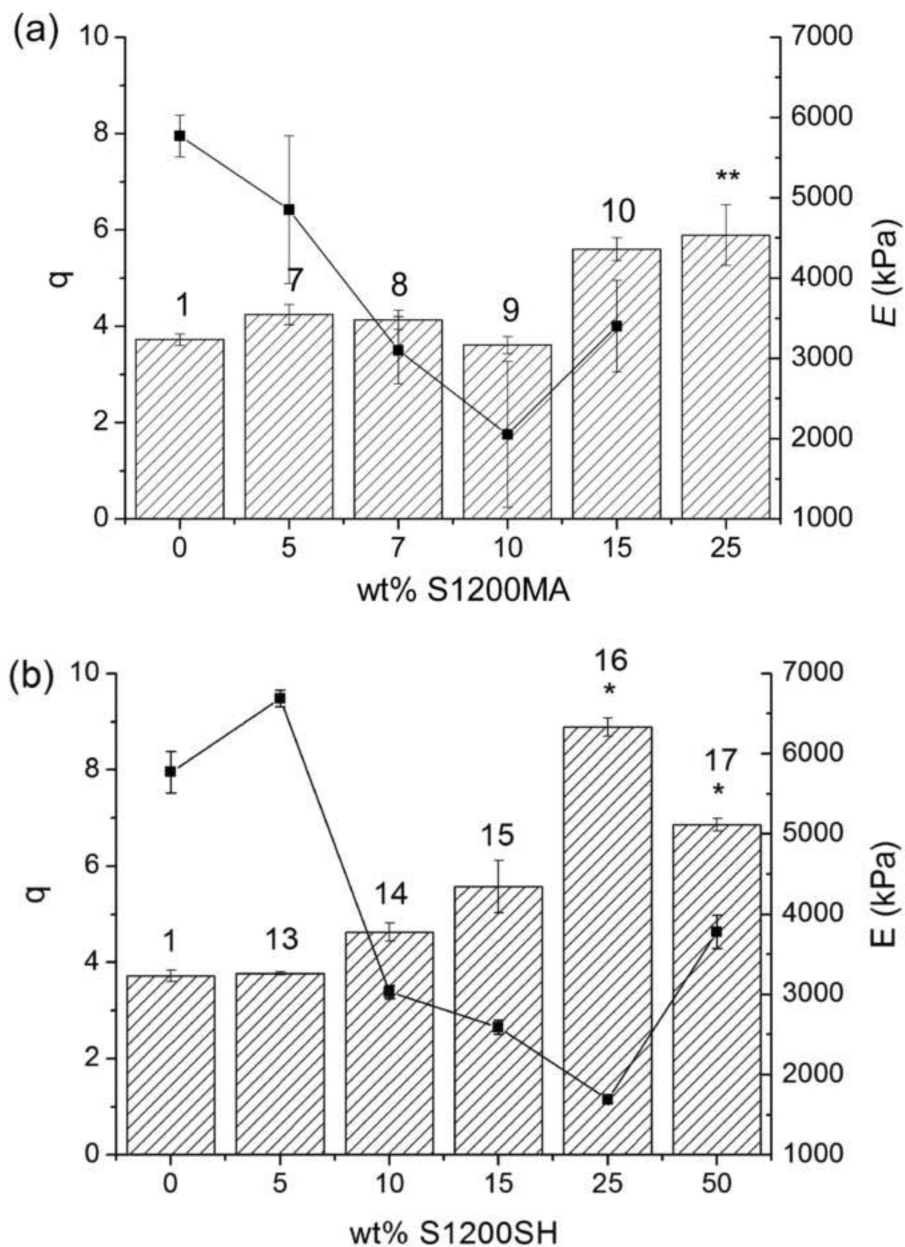
Figure 1.
Swelling ratio at the equilibrium, q (bars), and Young modulus, E (lines), of hydrogels based on PEGDA and S1200MA DS 5 (a) or S1200SH (b) in PBS pH 6.5. Error bars represent mean ± SD. Asterisks denote statistical significance (* $p<0.01$ and ** $p<0.05$) from the PEG700DA hydrogel. The number over each bar corresponds to the hydrogel number indicated in Table 1.
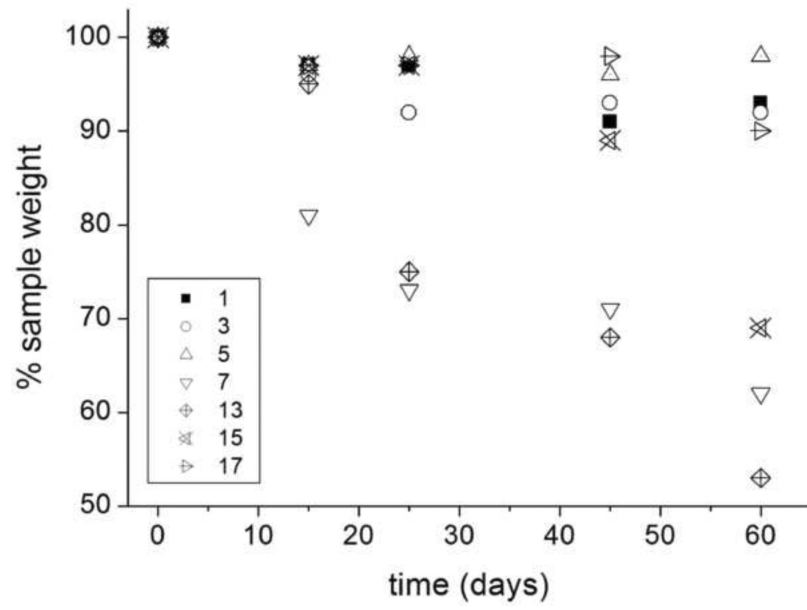
Figure 2.
Degradation profiles over time of PEGDA hydrogels with hyperbranchedpolymers
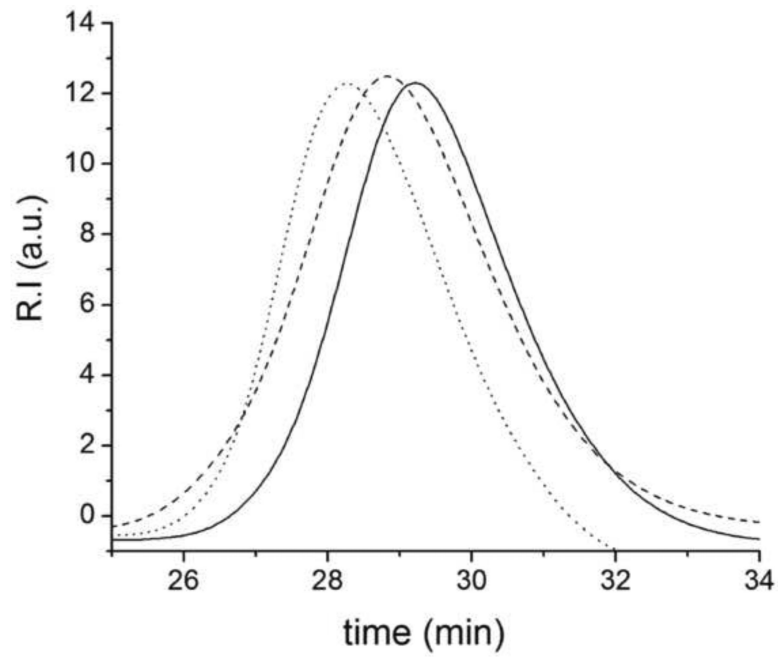S1200MA (**1, 3, 5** and **7**) and S1200SH (**13**, **15** and **17**).

Figure 3.
Elution chromatogram obtained for PEGacrylated-Hp (dotted line) and HpMA macromer (slashed line) compared to non-modified heparin profile (straight line). The normalized signals of refractive index detector are presented here versus time.
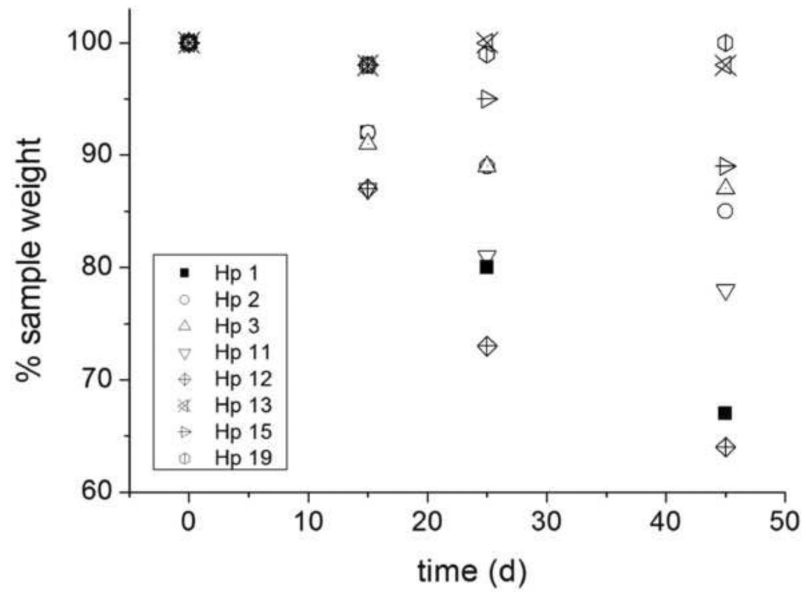
Figure 4.
Degradation profiles of PEGDA hydrogels with hyperbranched polymers S1200MA and S1200SH and bioconjugated with methacrylated heparin (HpMA). Values are normalized to hydrogel **1**.
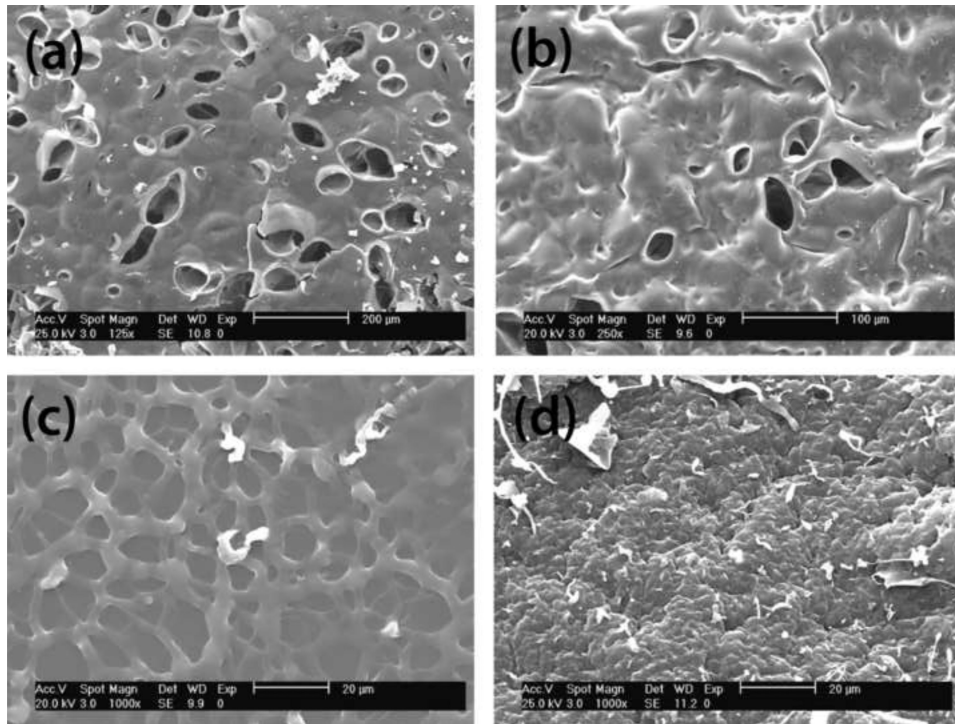
Figure 5.
SEM micrographs of the surface of bioconjugated Hp hydrogels: (a) **Hp12** (HpMA 10 mM / PEGDA and 5 wt% S1200MA DS 2); (b) **Hp15** (HpMA 10 mM /PEGDA and 15 wt% S1200MA DS 5); (c)**9** (10 wt% S1200MA DS 5) and (d) **Hp3**(HpMA 10 mM and PEGDA).
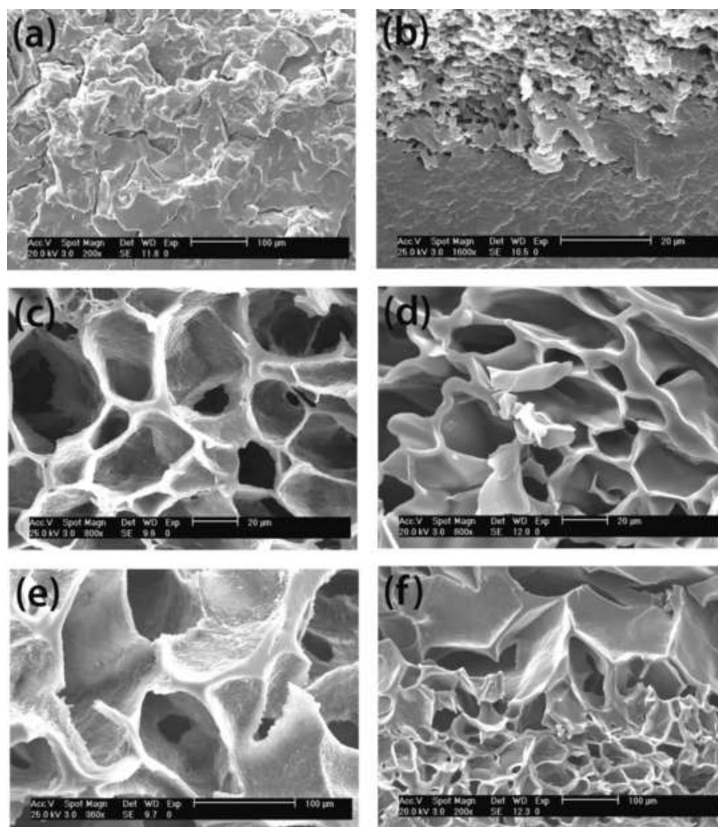
Figure 6.
SEM micrographs of the hydrogel sections. (a) hydrogel **3** (5 wt% S1200MA DS 2); (b) **Hp3** (10 mM HpMA); (c) **Hp12** (10 mM HpMA + 5 wt% S1200MA DS 2); (d) **Hp14** (1 mM HpMA+ 15 wt% S1200MA DS 5), (e) **Hp19** (10 mM HpMA + 5 wt% S1200SH), (f) **Hp15** (10 mM HpMA+ 15% wt S1200MA DS 5). Crosslinking densities are 5.7, 3.0, 1.4, 2.9, 3.3 and 4.4 respectively.
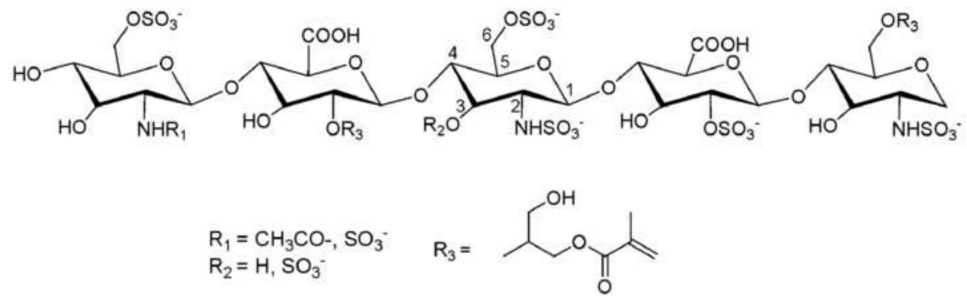
Scheme 1.
Heparin macromonomer HpMA obtained by reaction of heparin with glycidyl methacrylate. The most probable structure is shown.
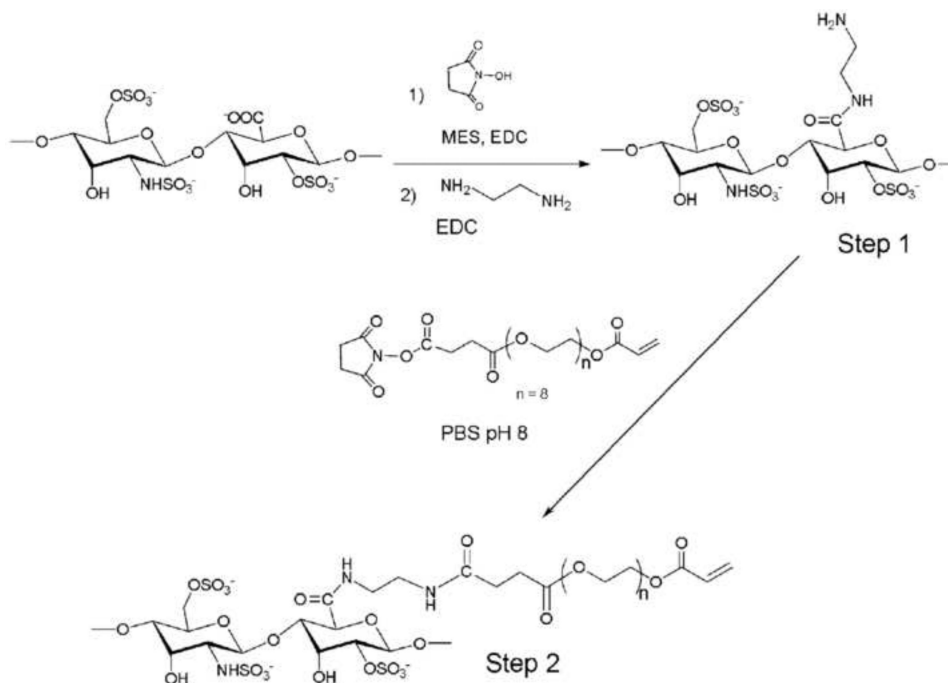
Scheme 2.
Heparin was previously modified with amine groups to obtain the pegylated-Hp macromonomer. Carboxylic acid groups are activated with NHS to react with ethylenediamide in Step 1. These newly formed amine groups couple with the activated carboxylic groups of the poly(ethylene glycol) acrylate (Step 2).
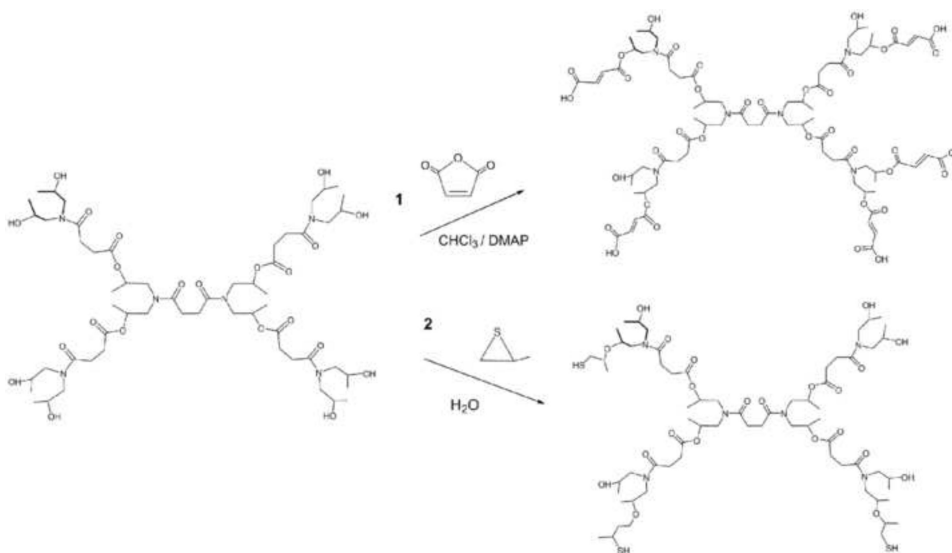
Scheme 3.
Representation of the derivatization of hyperbranched polymer S1200 with maleic acid and thiol functional groups.

Table 1

Composition and concentration of crosslinkable and total reactive groups in the precursor formulation of hydrogels. They are based on PEGDA and modified hyperbranched macromer S1200 with different degrees of substitution. Crosslinking density, calculated from mechanical data (ν_e) is also shown here.

	DS of HBP	HBP (wt%)	Fumaric (mM)	Thiol (mM)	Acrylate (mM)	Total (M)	$\nu_e \times 10^4$ (mol/cm^3)
1	-	0	-	-	355	710	7.8
2 [a]	-	0	-	-	65	130	0.6
3	2	5	10	-	340	700	5.7
4	2	10	20	-	321	680	4.6
5	2	15	30	-	305	670	3.4
6	5	2	13	-	350	716	3.3
7	5	5	33	-	340	721	6.5
8	5	7	47	-	332	723	4.2
9	5	10	67	-	321	727	2.8
10	5	15	100	-	305	735	4.6
11 [a]	2	10	20	-	60	160	0.4
12 [a]	2	15	30	-	55	170	0.5
13 [b]	2	5	-	10	340	700	9.0
14 [b]	2	10	-	20	321	680	4.1
15 [b]	2	15	-	30	305	670	3.5
16 [b]	2	25	-	50	270	640	2.3
17 [b]	2	50	-	100	180	560	5.1

[a] PEGDA (M$_n$4000 Da), while M$_n$ 700 is used for the rest

[b] HBP is S1200SH while S1200MA is used in 3 to **7**.

Table 2

Characteristics of heparin-containing hydrogels based on PEGDA (M_n 700 Da) and S1200MA with different degree of substitution (DS). Composition of precursor formulations, compressive modulus (E) and degree of swelling at pH 6.5 (q) are listed here. In hydrogels **Hp8, Hp9** and **Hp10**, PEGA-Hp was used instead of HpMA.

Hydrogel	DS	wt% HBP	Heparin (mM)	E (kPa)	q
Hp1	-	0		4328 ± 77	3.3 ± 0.6
Hp2	-	0	1	4556 ± 25	3.5 ± 0.4
Hp3	-	0	10	2245 ± 21	6.6 ± 0.1
Hp4 [a]	-	0	0.1	444 ± 59	6.6 ± 0.7
Hp5 [a]	-	0	1	371 ± 10	5.3 ± 1.5
Hp6 [a]	-	0	10	117 ± 12	8.5 ± 1.2
Hp7 [a]	-	0	20	85 ± 10	11.9 ± 0.7
Hp8 [a]	-	0	0.1	472 ± 37	6.1 ± 0.4
Hp9 [a]	-	0	1	395 ± 15	7.1 ± 0.2
Hp10 [a]	-	0	10	360 ± 6	5.1 ± 0.5
Hp11	2	5	5	2565 ± 403	4.5 ± 0.02
Hp12	2	5	10	1014 ± 82	9.7 ± 0.3
Hp13	5	15	0.1	2375 ± 134	5.3 ± 0.1
Hp14	5	15	1	2160 ± 506	26.1 ± 2.3
Hp15	5	15	10	3260 ± 406	6.6 ± 0.7
Hp16 [a]	2	10	0.1	201 ± 12	8.8 ± 1.2
Hp17 [a]	2	10	1	253 ± 21	7.4 ± 0.5
Hp18 [a]	2	10	10	191 ± 36	20.9 ± 3.4
Hp19 [b]	2	10	10	2443 ± 376	6.8 ± 0.7

[a] PEGDA (M_n 4000 Da)

[b] S1200SH is used instead of S1200MA

Table 3

Swelling behavior of hydrogels with 15 wt% S1200MA (hydrogel **5** with DS 2 and hydrogel **10**, DS 5) and 15 wt% S1200SH (hydrogel **15**).

Hydrogel	pH	% Swelling ratio at t = 10 min	% Swelling ratio at t = 100 min	% Swelling ratio at t = 1000 min
5	6.5	225 ± 18	333 ± 10	315 ± 22
10	6.5	454 ± 20	451 ± 11	490 ± 10
15	6.5	400 ± 16	413 ± 8	497 ± 15
5	8.0	202 ± 12	139 ± 5	169 ± 5
10	8.0	364 ± 25	305 ± 15	257 ± 8
15	8.0	1111 ± 62	1079 ± 71	1195 ± 55

Table 4

Comparison of swelling behavior of a bioconjugated hydrogel, **Hp15**, and a non-bioconjugated one, **10**, as a function of time at two different pH values.

Hydrogel	pH	% Swelling ratio at t = 10 min	% Swelling ratio at t = 100 min	% Swelling ratio at t = 1000 min
10	6.5	450 ± 40	450 ± 10	490 ± 10
Hp15	6.5	300 ± 30	310 ± 20	370 ± 20
10	8.0	360 ± 20	300 ± 20	260 ± 10
Hp15	8.0	520 ± 30	390 ± 30	530 ± 20